Histol Histopathol (2021) 36: 207-216

http://www.hh.um.es

Histology and Histopathology
From Cell Biology to Tissue Engineering

ORIGINAL ARTICLE **Open Access**

Overexpression of hsa_circ_0094742 inhibits IL-1β-induced decline in CHON-001 cell viability by targeting microRNA-127-5p

Mingqi Sun[1]*, Junli Yang[2]*, Dianming Jiang[3] and Guoyu Bao[1]

[1]Department of Orthopaedic Trauma, the Second Affiliated Hospital of Inner Mongolia Medical University, Huhhot, [2]Physical Examination Center, the Affiliated Hospital of Inner Mongolia Medical University, Inner Mongolia and [3]Department of Orthopedics, the First Affiliated Hospital of Chongqing Medical University, Chongqing, China

*These authors equally contribute to this study

Summary. Osteoarthritis (OA) is a public health problem that affects 240 million people globally; however, the current treatment options for OA are not effective. Therefore, there is still an urgent need to identify novel strategies to reduce the incidence and progression of OA. The circular RNA hsa_circ_0094742 was reported to be downregulated in patients with OA. However, the underlying mechanism remains unclear. The levels of hsa_circ_0094742 in CHON-001 were detected by reverse transcription quantitative polymerase chain reaction. Moreover, Cell Counting Kit-8 assay and Ki67 staining were used to determine the cell viability. The protein expression of biomarkers was detected by western blot analysis. In addition, the putative downstream target of hsa_circ_0094742 was predicted using the Circinteractome and TargetScan online databases. The putative targeting relationship was verified by dual luciferase reporter assay and fluorescence in situ hybridization. Next, cell apoptosis was determined by Annexin V/PI staining. hsa_circ_0094742 overexpression (OE) inhibited interleukin (IL)-1β-induced decline in the viability of CHON-001 cells and primary human chondrocytes. Furthermore, IL-1β-induced alterations in aggrecan, matrix metallopeptidase 13, X-linked inhibitor of apoptosis protein (XIAP), Bax and active caspase 3 were reversed by hsa_circ_0094742 OE. Luciferase reporter assay indicated that miR-127-5p was the downstream target of hsa_circ_0094742, and latexin was the target of miR-127-5p. hsa_circ_0094742 OE inhibited IL-1β-induced decline in CHON-001 cell viability by targeting miRNA-127-5p. The findings of the present study revealed the biological rational of the use of hsa_circ_0094742 OE as an anti-IL-1β effector in human chondrocytes. These findings may prompt further research on hsa_circ_0094742 as a potent circRNA target for the treatment of OA.

Key words: Osteoarthritis, hsa_circ_0094742, miR-127-5p, LXN

Introduction

Osteoarthritis (OA) results from the degenerative changes in the joint cartilage (Nelson, 2018). To date, OA remains a public health problem, affecting 240 million people globally (Nelson, 2018). The prevalence of OA in China is high (Tang et al., 2016). According to data from the China Health and Retirement Longitudinal Study, the prevalence of symptomatic knee OA in China is as high as 8% (Tang et al., 2016). OA is accompanied by disability and reduced quality of life, and is a

Corresponding Author: Dianming Jiang, Department of Orthopedics, the First Affiliated Hospital of Chongqing Medical University, No.1 Youyi Road, Chongqing 400016, China. e-mail: dianming.jiang@yandex.com or Guoyu Bao, Department of Orthopaedic Trauma, the Second Affiliated Hospital of Inner Mongolia Medical University, No.1 Yingfangfao Road, Huhhot, Inner Mongolia 010030, China. e-mail: guoyubao5272@126.com

DOI: 10.14670/HH-18-325

Abbreviations. ATCC, American Type Culture Collection; BCA, bicinchoninic acid; CCK-8, Cell counting kit-8; circRNAs, circular RNAs; ECL, chemiluminescence; ECM, extracellular matrix; FISH, fluorescence in situ hybridization; IGF1R, insulin-like growth factor 1 receptor; IL-1β, interleukin-1β; LXN, Latexin; miR-127-50, microRNA-127-5p; MMP-13, Matrix metallopeptidase 13; NAMPT, nicotinamide phosphoribosyl transferase; NSAIDs, nonsteroidal anti-inflammatory Drugs; OA, osteoarthritis; OE, overexpression; PVDF, polyvinylidene difluoride; RT-qPCR, quantitative real-time polymerase chain reaction; Rps3, ribosomal protein subunit 3; SDS-PAGE, sodium dodecyl sulfate polyacrylamide gel electrophoresis

contributing factor to mortality (Nelson, 2018). Treatment options for OA include weight loss, exercise, oral and topical nonsteroidal anti-inflammatory drugs, and intra-articular treatments (Tang et al., 2016). Despite these treatment options, the lack of effective treatment strategies is a factor contributing to the continuing increase in the worldwide prevalence of OA (Nelson, 2018). Therefore, there is still an urgent need to explore novel strategies for the reduction of the incidence and progression of OA (Nelson, 2018).

Circular RNAs (circRNAs) are a class of endogenous RNAs with a complete ring structure formed by covalently joining the 3' and 5' ends (Qu et al., 2015; Li et al., 2019). It has been proven that circRNAs play a critical role in regulating gene expression at the post-transcriptional level (Zhao et al., 2018). Specifically, circRNAs act as competing endogenous RNAs to bind with the targeted microRNAs (miRNAs), thereby inhibiting their activity (Shu et al., 2019). A previous study has proven that circRNAs participate in multiple physiological activities (Braicu et al., 2019). Moreover, the dysregulation of circRNAs is involved in the pathogenesis of several diseases, such as neurological disorders (Li et al., 2017b), cardiovascular disease (Fan et al., 2017), cancer (Kristensen et al., 2018), acute kidney injury (Brandenburger et al., 2018), type II diabetes (Haque and Harries, 2017), pre-eclampsia (Haque and Harries, 2017), OA (Haque and Harries, 2017), etc. A previous study showed that hsa_circ_0094742 was downregulated in the cartilage of patients with OA (Wang et al., 2019). However, further biological research revealing the underlying mechanisms is still lacking. The aim of the present study was to explore the role of hsa_circ_0094742 in cartilage cells *in vitro*, and to reveal the underlying mechanisms.

Materials and methods

Cell culture

CHON-001 immortalized cartilage cells were obtained from the American Type Culture Collection (ATCC; #CRL-2846) and maintained in Dulbecco's modified Eagle's medium (Thermo Fisher Scientific, Inc.) containing fetal bovine serum (10%), streptomycin (100 mg/ml) and penicillin (100 U/ml) at 37°C in a humidified incubator with 5% CO_2. Primary human articular chondrocytes were purchased from ScienCell Research Laboratories and cultured in Chondrocyte Medium (ScienCell Research Laboratories) in a humidified incubator with 5% CO_2. CHON-001 cells and human articular chondrocytes were stimulated with interleukin (IL)-1β (10 ng/ml; Sigma-Aldrich) for 24 h to mimic OA *in vitro*.

Overexpression (OE) of hsa_circ_0094742

Hsa_circ_0094742 overexpressing vectors were constructed by GenePharma. In addition, the lentiviruses were packaged and purified by GenePharma. For the lentiviral infections, CHON-001 cells were seeded onto 6-well plates. The next day, the cells were infected with hsa_circ_0094742 overexpressed lentiviruses. After 48 h of culture, stable strains were selected with 5 μg/ml puromycin. The expression of hsa_circ_0094742 was confirmed by reverse transcription quantitative polymerase chain reaction (RT-qPCR).

Cell transfection

Negative control (NC) and miR-127-5p agomir were synthesized by GenePharma. The cells were transfected with miR-127-5p agomir or NC for 48 h using Lipofectamine® 2,000 reagent (Thermo Fisher Scientific, Inc.), following the manufacturer's instructions. Next, the cells were exposed to IL-1β for 24 h. The efficiency of transfection was determined using RT-qPCR 48 h after cell transfection.

RT-qPCR

Total RNA was isolated from CHON-001 cells using TRIzol® reagent (Thermo Fisher Scientific, Inc.) and transcribed into cDNA using the PrimeScript RT Reagent Kit (Takara Bio, Inc.). RT-qPCR (CFX 96; thermocycler; Bio-Rad Laboratories, Inc.) was performed on an Applied Biosystems 7500HT system (Thermo Fisher Scientific, Inc.) to detect the expression of genes using the SYBR Premix Ex TaqIIKit (Takara Bio, Inc.). Actin and U6 were used as endogenous controls for the quantification of genes. The relative expression levels of genes were calculated using the $2^{-\Delta\Delta Cq}$ method. Primer sequences were as follows: hsa_circ_0094742, 5'- GACCCTGGCAAGTGT GAGAAC-3' forward and 5'-GTAACGAAGGTGG TACCTGCG-3' reverse; miR-127-5p, 5'-CTGAAGCT CAGAGGGCTCTG-3' forward and 5'-CTCAACTG GTGTCGTGGAGTC-3' reverse; LXN, 5'-CACAGG GTGTTTGAGGTGCA-3' forward and 5'-GCTTCT AGCGGTTCCTTCATG-3' reverse; U6, 5'-CTCGC TTCGGCAGCACAT-3' forward and 5'-AACGCTT CACGAATTTGCGT-3' reverse; Actin, 5'-GTCCAC CGCAAATGCTTCTA-3' forward and 5'-TGCTGTCA CCTTCACCGTTC-3' reverse.

Cell Counting Kit-8 (CCK-8) assay

CCK-8 assay was performed to determine cell viability, according to the manufacturer's instructions. A total of $5x10^3$ cells were seeded in 96-well plates overnight. Following treatment, the cells were incubated with 10 µl CCK-8 reagent for 3h at 37°C. Absorbance was measured at 450 nm using a spectrophotometer at the indicated time points.

Immunofluorescence analysis

CHON-001 cells were seeded on slides and

indicated treatments were performed. Following treatment, the cells were washed with PBS twice and fixed with 4% paraformaldehyde for 30 min at 4°C. The cells were then permeabilized with 0.1% Triton X-100 and blocked with 3% BSA at room temperature for 5 min. Subsequently, cells were incubated with primary antibodies against Ki67 (1:300; Abcam) overnight at 4°C. Following washing with PBS three times, cells were incubated with secondary antibody for 1 h at room temperature. The cell nuclei were counterstained with DAPI (1 mg/ml; Sangon Biotech Co., Ltd.). Images were acquired by fluorescence microscopy (Carl Zeiss AG).

Apoptosis assay

Annexin V-FITC Apoptosis Kits (BD Biosciences) were used to determine cell apoptosis, following the manufacturer's instructions. The cells were harvested and resuspended at a density of $5x10^6$ cells/ml after the indicated treatment. Cells were then stained with Annexin V-FITC/PI and subjected to flow cytometry.

Western blot analysis

Total protein was acquired with RIPA buffer (Beyotime Institute of Biotechnology) and quantified using a bicinchoninic acid protein assay kit (Beyotime Institute of Biotechnology). Equal amounts of protein were subjected to sodium dodecyl sulfate polyacrylamide gel electrophoresis and transferred onto a polyvinylidene difluoride (PVDF) membrane. Next, PVDF membranes were blocked with 5% skimmed milk for 2 h, followed by incubation with primary antibodies at 4°C overnight. Following washing with 1x TBST three times, the membranes were incubated with anti-rabbit secondary antibodies (horseradish peroxidase-conjugated 1:2,000) at room temperature for 2h. The intensity of immunoreactive bands was determined using an enhanced chemiluminescence kit (Beyotime Institute of Biotechnology). β-actin was used as the loading control. Primary antibodies against aggrecan (1:1,000), matrix metallopeptidase 13 (MMP13) (1:1,000), XIAP (1:1,000), Bax (1:1,000), active caspase 3 (1:1,000), LXN (1:1,000), ribosomal protein subunit 3 (Rps3; 1:1,000) and β-actin (1:1,000) were obtained from Abcam.

Dual luciferase reporter assay

The downstream target of hsa_circ_0094742 was predicted using the CircInteractome online database (https://circinteractome.nia.nih.gov/index.html). miR-127-5p was identified as the direct target of hsa_circ_0094742. Next, the downstream target of miR-127-5p was predicted using TargetScan (www.targetscan.org/vert_71) and miRWalk (http://zmf.umm.uni-heidelberg.de/apps/zmf/mirwalk/micrornapredictedtarget.html).

Subsequently, dual luciferase reporter assay was used to investigate the potential binding relationship between miR-127-5p and target proteins. Specifically, the wild type (WT) and mutant (MT) 3' UTR of hsa_circ_0094742 were cloned into pmiR-RB-Report™ vectors (Guangzhou RiboBio Co., Ltd.), following the manufacturer's instructions. CHON-001 cells were co-transfected with luciferase reporter vector and miR-127-5p agomir or NC using Lipofectamine® 2000 reagent (Thermo Fisher Scientific, Inc.) at 37°C for 48 h. In addition, to verify the binding relationship between miR-127-5p and LXN, the WT and MT 3'UTR of LXN were cloned into pmiR-RB-Report™ vectors (Guangzhou RiboBio Co., Ltd.), following the manufacturer's instructions. CHON-001 cells were co-transfected with luciferase reporter vector and miR-127-5p agomir or NC using Lipofectamine® 2000 reagent (Thermo Fisher Scientific, Inc.) at 37°C for 48 h. Dual-luciferase Assay System (Promega Corporation) was used to determine the luciferase activity, following the manufacturer's instructions.

Fluorescence in situ hybridization (FISH)

FISH was performed using a fluorescence in situ hybridization kit (Guangzhou RiboBio Co., Ltd.), following the manufacturer's instructions. Hsa_circ_0094742 and miR-127-5p probes were designed and synthesized by the RiboBio Company. In brief, the cells were collected following the indicated treatment for 48 h and seeded on glass slides. They were then fixed with 4% paraformaldehyde for 10 min, followed by permeabilization with 0.5% Triton X-100 at 4°C for 10 min. Following washing with PBS three times, the cells were pre-hybridized at 37°C for 30 min. Hybridization was performed by incubation at 37°C overnight in the dark. In addition, the cells were counterstained with DAPI, washed three times with PBS, and visualized using a confocal microscope (BX41; Olympus Corporation).

Statistical analysis

All statistical analysis was performed using GraphPad Prism 7 (GraphPad Software, Inc.). All experiments were repeated at least in triplicate and are presented as the mean ± SD. One-way ANOVA followed by a Tukey's test was used to compare more than two groups. $P<0.05$ was considered to indicate a statistically significant difference.

Results

Hsa_circ_0094742 OE ameliorated IL-1β-induced proliferation inhibition in CHON-001 cells

CHON-001 cells were first stimulated with IL-1β to mimic the OA state *in vitro*. Since the downregulation of hsa_circ_0094742 in patients with OA had been previously reported (Wang et al., 2019),

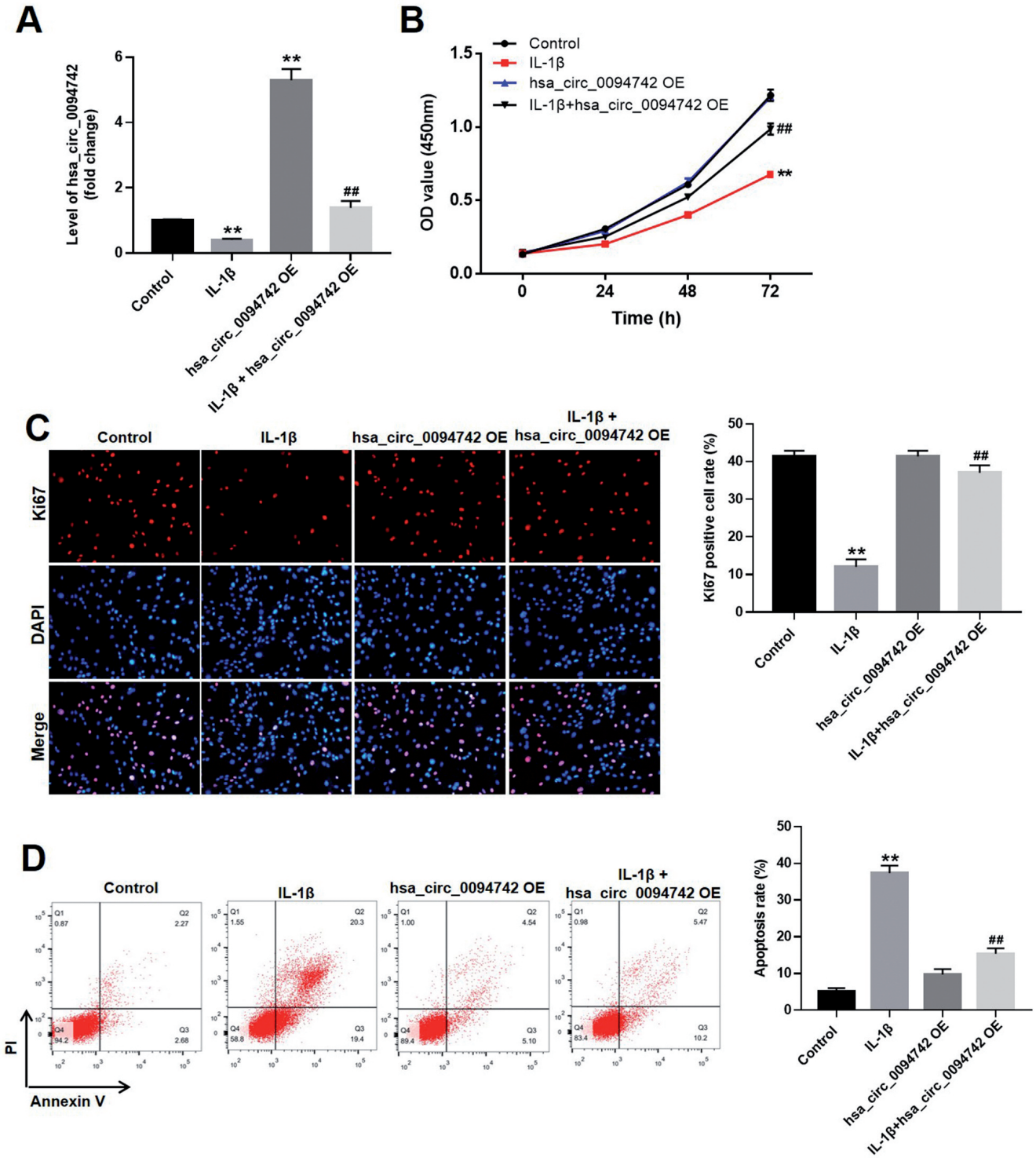

Fig. 1. Hsa_circ_0094742 OE ameliorated IL-1β-induced cell proliferation inhibition in CHON-001 cells. CHON-001 cells were infected with hsa_circ_0094742 OE for 48h, followed by stimulated with 10 ng/ml IL-1β for 24h. **A.** The efficiency of hsa_circ_0094742 OE was verified by RT-qPCR. **B.** Cell viability was evaluated by CCK-8 assay at indicated time points. **C.** Immunofluorescence staining of Ki67 was performed to detect the proliferation of CHON-001 cells in each group. Ki67 positive cells were counted. **D.** Annexin V/PI staining was conducted to detect cell apoptosis. The apoptosis rate in each group was quantified. **P<0.01, compared with control group; ##P<0.01, compared with IL-1β treated group. n=3.

hsa_circ_0094742 OE was induced in CHON-001 cells in the present study. As shown in Fig. 1A, hsa_circ_0094742 was downregulated in the IL-1β-treated group, as compared with that in the control group. Furthermore, hsa_circ_0094742 OE (hsa_circ_0094742 OE) significantly increased the level of hsa_circ_0094742 in CHON-001 cells. However, the upregulation of hsa_circ_0094742 was clearly inhibited in the presence of IL-1β (Fig. 1A). Next, CCK-8 assay was performed to investigate the effect of hsa_circ_0094742 OE on the viability of CHON-001 cells. As shown in Fig. 1B, hsa_circ_0094742 OE clearly reversed the IL-1β-induced cell viability decrease in CHON-001 cells. Consistently, the result of immunofluorescence staining indicated that hsa_circ_0094742 OE alleviated the IL-1β-induced proliferation decline in CHON-001 cells (Fig. 1C). Furthermore, the apoptosis assay results indicated that IL-1β-induced cell apoptosis was inhibited by hsa_circ_0094742 OE (Fig. 1D). All these results demonstrated that the OE of hsa_circ_0094742 could ameliorate IL-1β-induced proliferation inhibition in CHON-001 cells.

Hsa_circ_0094742 OE reverses IL-1β-induced protein alterations

The expression of OA and apoptosis-related biomarkers was detected by western blot analysis (Fig. 2A). The results illustrated that IL-1β decreased the expression of aggrecan and XIAP, and increased that of MMP-13, Bax and active caspase 3 in CHON-001 cells

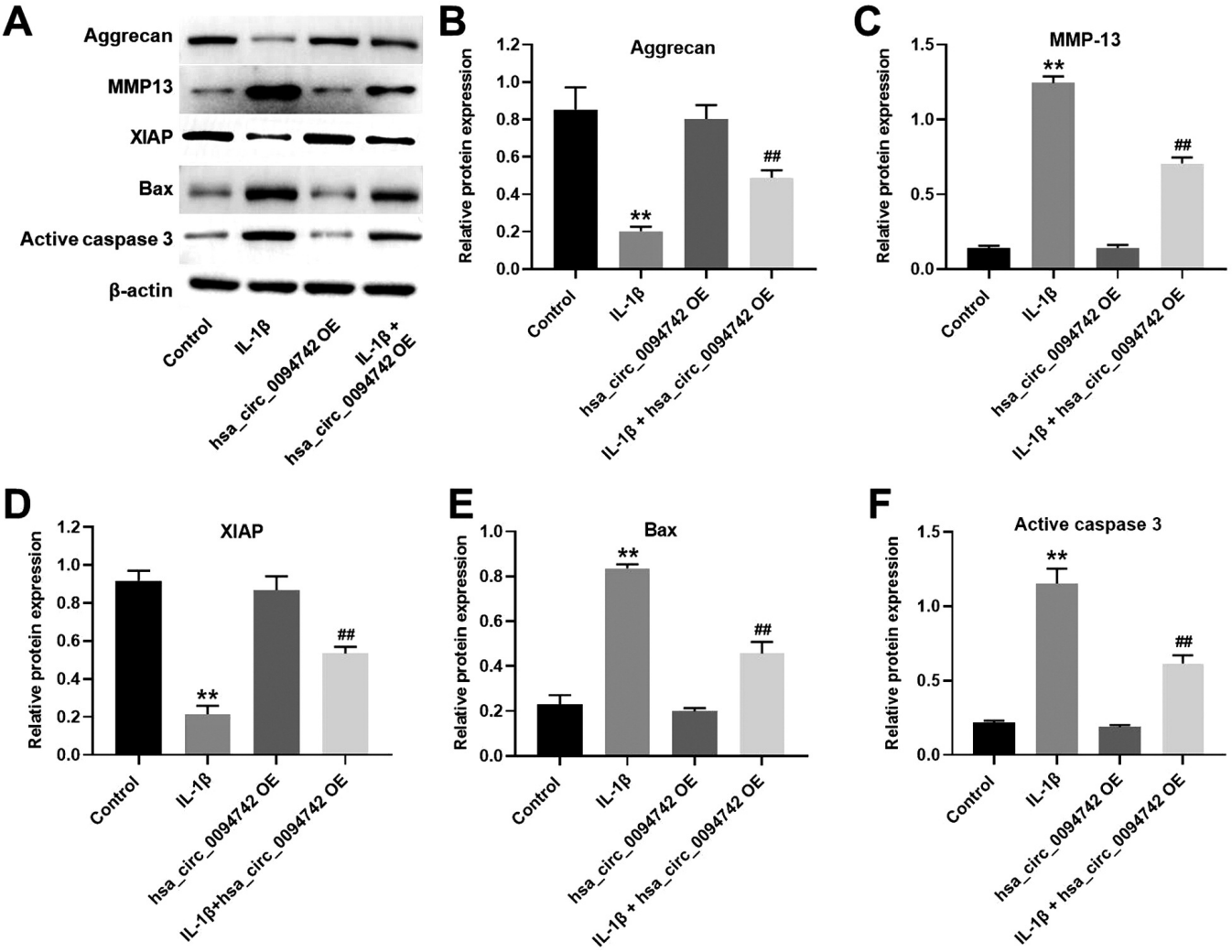

Fig. 2. Hsa_circ_0094742 OE reversed IL-1β-induced proteins alternations. CHON-001 cells were infected with hsa_circ_0094742 OE for 48h, followed by stimulated with 10 ng/ml IL-1β for 24h. **A.** Western blot was employed to detect the expressions of aggrecan, MMP13, XIAP, Bax and active caspase 3. β-actin was used as inner control. **B-F.** The relative expressions of aggrecan, MMP13, XIAP, Bax and active caspase 3 were quantified. **P<0.01, compared with control group; ##P<0.01, compared with IL-1β treated group. n=3.

(Fig. 2B-F); however, these phenomena were significantly reversed by hsa_circ_0094742 OE (Fig. 2B-F). These data indicated that hsa_circ_0094742 OE could reverse IL-1β-induced protein alternations.

miR-127-5p is the target of hsa_circ_0094742

Next, the Circinteractome online database was used to predict the downstream miRNA target of hsa_circ_0094742. The prediction result indicated that miR-127-5p was one of the most likely putative targets of hsa_circ_0094742 (Fig. 3A). Furthermore, miR-127-5p was previously found to regulate the proliferation of human chondrocytes and mediate the expression of MMP-13 (Park et al., 2013; Tu et al., 2016). Therefore, the following experiments attempted to verify the targeting relationship between hsa_circ_0094742 and miR-127-5p. Before verifying the potential targeting relationship between hsa_circ_0094742 and miR-127-5p, CHON-001 cells were transfected with miR-127-5p agomir or NC. The level of miR-127-5p was quantified by RT-qPCR to measure the efficiency of transfection

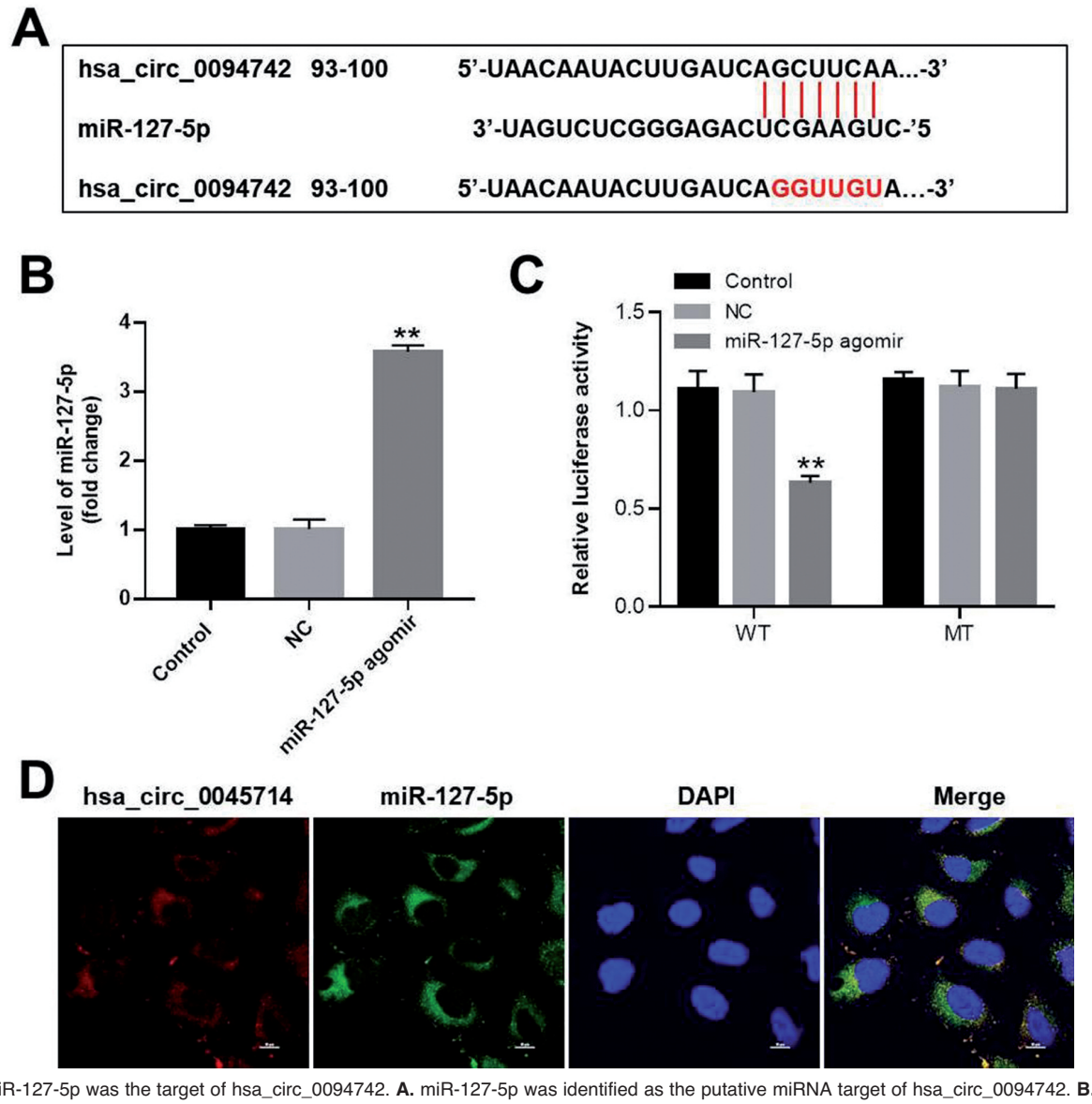

Fig. 3. miR-127-5p was the target of hsa_circ_0094742. **A.** miR-127-5p was identified as the putative miRNA target of hsa_circ_0094742. **B.** miR-127-5p agomir or vector control was transfected into CHON-001 cells for 48h. The efficiency of transfection was verified by RT-qPCR. **P<0.01, compared with control group. **C.** The targeting relationship between miR-127-5p agomir and hsa_circ_0094742 was verified by dual luciferase reporter assay. **D.** FISH assay was conducted to verify the targeting relationship between miR-127-5p and hsa_circ_0094742. **P<0.01, compared with control group. n=3.

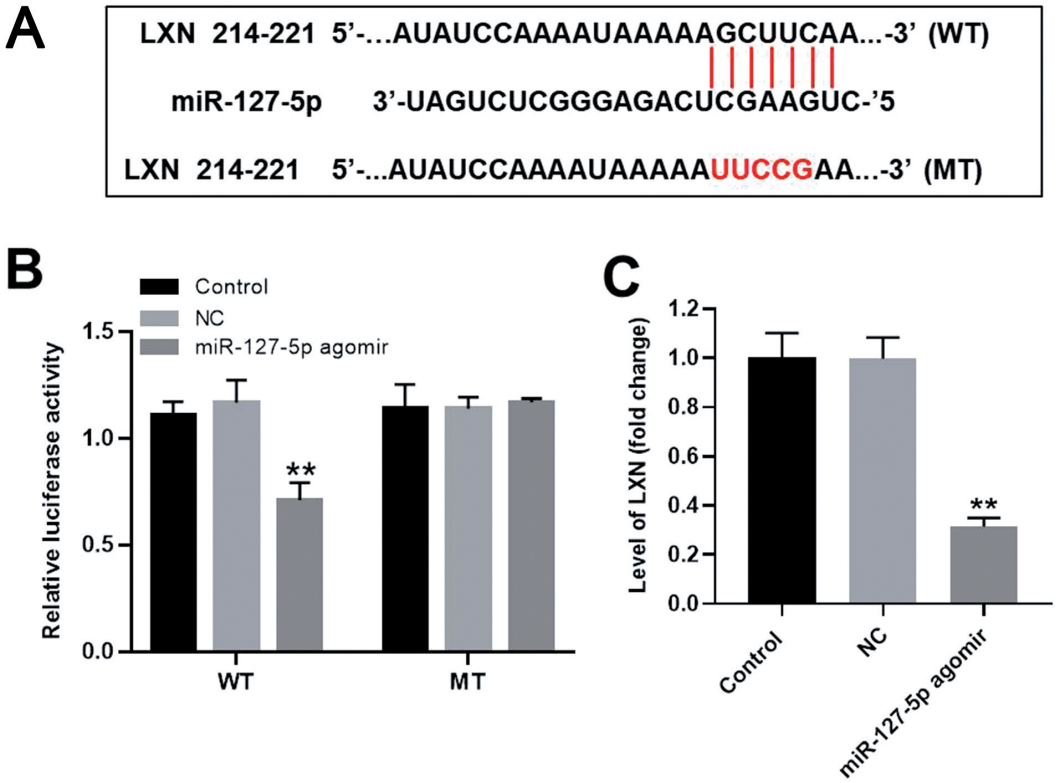

Fig. 4. LXN was the target of miR-127-5p. **A.** LXN was predicted the target of miR-127-5p. miR-127-5p agomir or vector-control was transfected into CHON-001 cells for 48h. **B.** The targeting relationship between LXN and miR-127-5p agomir was verified by dual luciferase reporter assay. **C.** The level of LXN was quantified by RT-qPCR. **P<0.01, compared with control group. n=3.

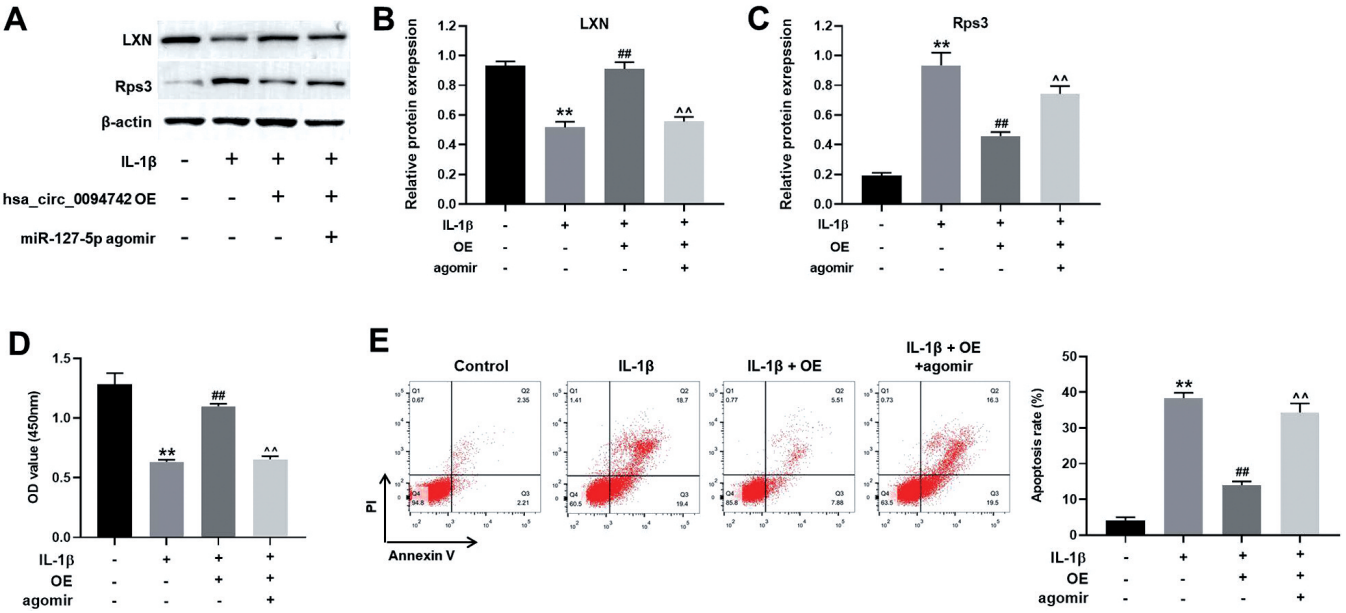

Fig. 5. Hsa_circ_0094742 OE protected CHON-001 cells against IL-1βthrough targeting miR-127-5p. The cells were treated with hsa_circ_0094742 overexpressed lentiviruses or/and mir-127-5p agomir for 48h, following exposure to IL-1β for 24h. The expression of LXN and Rps3 were detected by western blot. β-actin was used as inner control. **B, C.** The level of LXN and Rps3 were quantified. **D.** The cell viability in each group was evaluated by CCK-8 assay. **F.** The apoptosis rate in each group was determined by Annexin V/PI staining. **P<0.01, compared with control group; ##P<0.01, compared with IL-1β treated group; ^^P<0.01, compared with hsa_circ_0094742 OE group. n=3.

(Fig. 3B). After 48 h of transfection, dual luciferase reporter assay was performed. As illustrated in Fig. 3C, miR-127-5p agomir could notably inhibit the luciferase activity of WT hsa_circ_0094742, while it had no effect on MUT hsa_circ_0094742. In addition, FISH assay confirmed that hsa_circ_0094742 and miR-127-5p were co-located in the cytoplasm (Fig. 3D). These outcomes verified miR-127-5p as the target of hsa_circ_0094742.

Latexin (LXN) is the target of miR-127-5p

miRNAs regulate gene expression post-transcriptionally by binding to the 3'-UTR of their target mRNAs and repress protein production by mRNA destabilization and translational silencing (Jackson and Standart, 2007). Thus, the downstream protein target of miR-127-5p was predicted by TargetScan and miRWalk. Based on these databases, LXN was predicted as the putative target of miR-127-5p (Fig. 4A). Moreover, LXN was previously reported as an OA-associated protein (Jackson and Standart, 2007). We therefore focused on the analysis of LXN as a potential target of miR-127-5p in the following experiments. According to the dual luciferase reporter assay results, LXN was confirmed as the target of miR-127-5p (Fig. 4B). In addition, the level of LXN in CHON-001 cells was detected by RT-qPCR. As shown in Fig. 4C, the level of LXN was inhibited by miR-127-5p agomir, which also validated the relationship between miR-127-5p and LXN. In combination, LXN was identified as the target of miR-127-5p.

Hsa_circ_0094742 OE protected CHON-001 cells against IL-1β by targeting miR-127-5p

To further explore the mechanism underlying the targeting relationship between hsa_circ_0094742 and miR-127-5p, CHON-001 cells were infected with

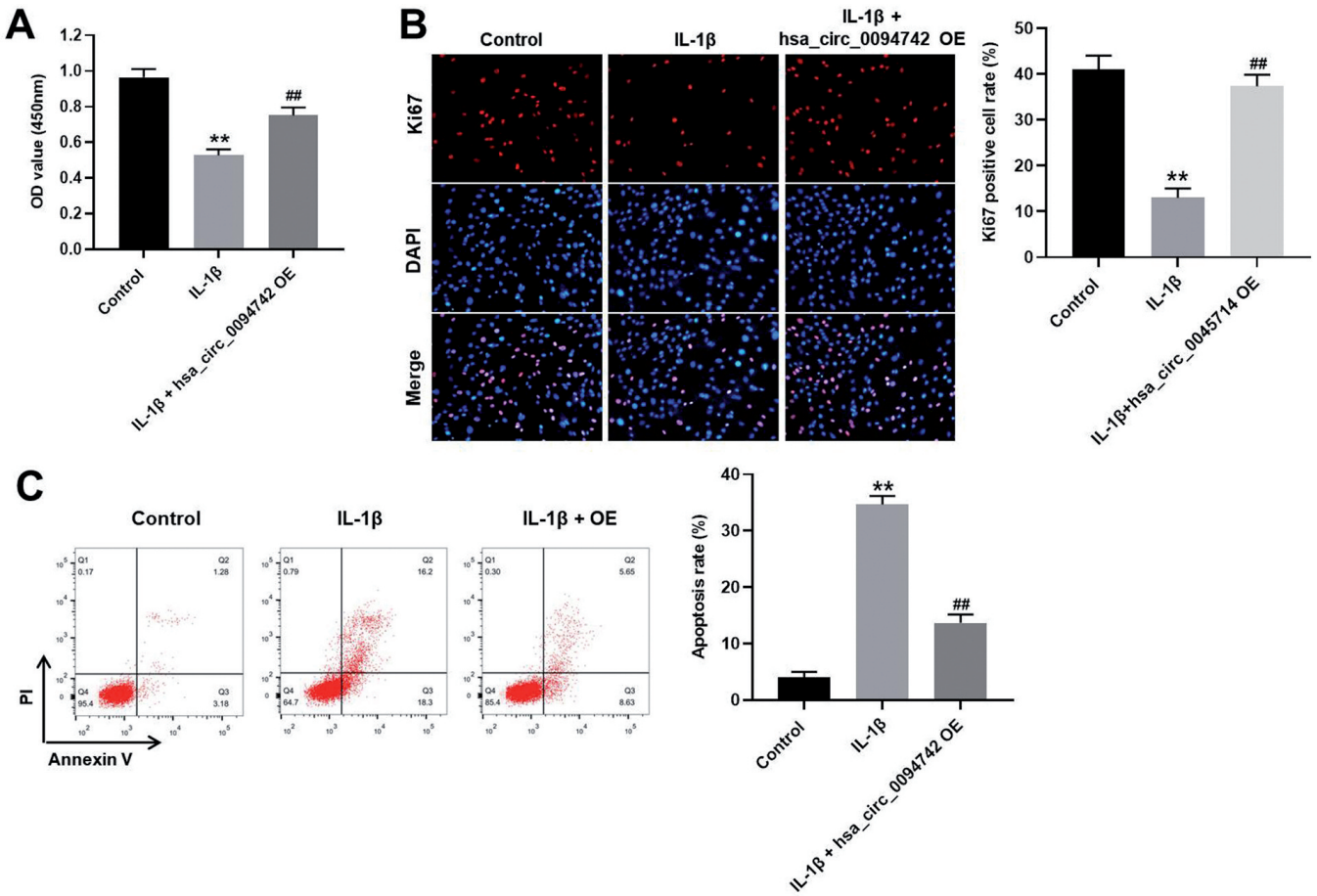

Fig. 6. Hsa_circ_0094742 OE ameliorated IL-1β-induced cell proliferation inhibition in primary human chondrocytes. Human chondrocytes were infected with hsa_circ_0094742 OE for 48h. Then, the cells were stimulated with 10 ng/ml IL-1β for 24h. **A.** Cell viability was evaluated by CCK-8 assay. **B.** Cell proliferation was determined by immunofluorescence staining of Ki67. Ki67 positive cells were counted. **C.** Annexin V/PI staining was utilized to detect cell apoptosis. The apoptosis rate in each group was quantified. **P<0.01, compared with control group; ##P<0.01, compared with IL-1β treated group. n=3.

hsa_circ_0094742 OE or/and miR-127-5p agomir for 48 h. Since Rps3 was previously reported as a binding protein of LXN (You et al., 2014), the level of LXN and Rps were detected by western blot analysis. As shown in Fig. 5A-C, IL-1β decreased the expression of LXN and increased that of Rps3. As expected, the effect of IL-1β on the alteration of LXN and Rps3 was reversed by hsa_circ_0094742 OE. Furthermore, the effect of hsa_circ_0094742 OE was abolished in the presence of miR-127-5p agomir. Furthermore, based on the result of the CCK-8 assay, the IL-1β-induced cell viability decrease was reversed by hsa_circ_0094742 OE (Fig. 5D). In the meantime, the effect of hsa_circ_0094742 OE on cell viability was abrogated by miR-127-5p agomir. IL-1β markedly induced cell apoptosis, which was reversed by hsa_circ_0094742 OE (Fig. 5E). Furthermore, the effect of hsa_circ_0094742 OE on cell apoptosis was abolished in the presence of miR-127-5p agomir. In combination, these results suggested that hsa_circ_0094742 OE protected CHON-001 cells against IL-1β by targeting miR-127-5p through the LXN/Rps3 pathway.

Hsa_circ_0094742 OE ameliorates IL-1β-induced cell proliferation inhibition in primary human chondrocytes

Since CHON-001 cells are immortalized cartilage cells instead of primary human chondrocytes, cell viability and apoptosis assays were performed again in primary human chondrocytes to verify the role of hsa_circ_0094742. As shown in Fig. 6A, IL-1β treatment resulted in the decreased viability of human chondrocytes. The IL-1β-induced viability decrease was ameliorated by hsa_circ_0094742 OE. Furthermore, the results of Ki67 staining also demonstrated that IL-1β led to a decline in the proliferation of human chondrocytes (Fig. 6B). The IL-1β-induced proliferation decline was ameliorated by hsa_circ_0094742 OE (Fig. 6B). Consistently, the apoptosis assay results illustrated that the IL-1β-induced cell apoptosis was alleviated by hsa_circ_0094742 OE (Fig. 6C). These results indicated that hsa_circ_0094742 OE retained its protective effect against IL-1β in primary human chondrocytes.

Discussion

At present, the treatment strategies for OA are limited and need to be improved (Nelson, 2018). Exploring new therapeutic targets would be useful for designing new treatment strategies against OA. Despite circRNAs emerging as potential therapeutic targets in human diseases, the involvement of circRNAs in the occurrence and development of OA has rarely been reported (Deng et al., 2019; Hu et al., 2019). A previous study by Wang et al reported that downregulation of hsa_circ_0094742 was observed in patients with OA, but did not explore the underlying mechanisms (Wang et al., 2019). In the present study, human chondrocytes were exposed to IL-1β stimulation to mimic OA conditions *in vitro*. hsa_circ_0094742 was found to be downregulated in IL-1β-stimulated CHON-001 cells, which was consistent with the findings of Wang et al. In addition, the effect of hsa_circ_0094742 OE on the cell proliferation of IL-1β-stimulated CHON-001 cells was further explored. The results of this study proved that hsa_circ_0094742 OE alleviated the decline in IL-1β-induced cell viability by targeting miR-127-5p through the LXN/Rps3 pathway. These findings were useful for identifying the molecular mechanisms through which hsa_circ_0094742 regulates the progression of OA. In combination with the findings of Wang et al, the present findings may prompt further research on hsa_circ_0094742 as a potential circRNA target for the treatment of OA. In line with the present findings, Zhou et al. reported that the upregulated circRNA.33186 promoted OA by directly targeting and sponging miR-127-5p (Zhou et al., 2019). Furthermore, Parra-Torres et al investigated the role of LXN expression in cartilage repair during the early stages of OA (Parra-Torres et al., 2014). These previous studies supported the present findings. However, this study was not without its limitations. Although miR-127-5p was verified as the target of hsa_circ_0094742, miR-127-5p may not be the only miRNA target of hsa_circ_0094742. Instead, a complex circRNA-miRNA-mRNA regulating network may be involved in the regulation of OA (Xiao et al., 2019).

In another previous study, Li et al. reported that hsa_circ_0045714 could regulate ECM synthesis, proliferation and apoptosis in chondrocytes by promoting the expression of miR-193b target gene insulin-like growth factor 1 receptor (IGF1R) (Li et al., 2017a). In contrast with our findings, Li et al reported that hsa_circ_0045714 OE exerted no effect on miR-193b expression (Li et al., 2017a,b). Moreover, hsa_circ_0045714 OE was found to inhibit the transcriptional activity of miR-193b, thereby upregulating the expression of IGF1R (Li et al., 2017a). However, in the present study, it was found that hsa_circ_0094742 OE had a direct effect on the level of miR-127-5p. These differences suggested that different circRNAs play a role in cellular physiology through multiple types of mechanisms (Ng et al., 2018). Common functioning mechanisms of circRNAs involve miRNA sponging, RNA-binding protein binding molecules, transcriptional regulators, immune regulators and templates for protein translation (Ng et al., 2018). Other mechanisms involved in the role of hsa_circ_0094742 in the progression of OA remain to be further explored.

In conclusion, hsa_circ_0094742 OE protected human chondrocytes from IL-1β by targeting miR-127-5p. The findings of the present study revealed the biological rationale of the use of hsa_circ_0094742 OE to protect human chondrocytes against IL-1β. These findings may prompt further research on hsa_circ_0094742 as a potential novel circRNA target for the treatment of OA.

Availability of data and materials. The datasets used and/or analysed during the current study are available from the corresponding author on reasonable request.

Conflict of interests. The authors declare that they have no conflict of interests.

Authors' contributions. MS and JY conceived this study, conducted part of experiments, and made substantive contribution to drafting the manuscript. DJ and GB were major contributors in data analysis and interpretation, as well as involved in the execution of experiments. All authors reviewed and approved the final draft of the manuscript prior to submission.

Funding. Inner Mongolia Natural Science Foundation (2019MS08158).

References

Braicu C., Zimta A.A., Gulei D., Olariu A. and Berindan-Neagoe I. (2019). Comprehensive analysis of circular RNAs in pathological states: biogenesis, cellular regulation, and therapeutic relevance. Cell Mol. Life Sci. 76, 1559-1577.

Brandenburger T., Salgado Somoza A., Devaux Y. and Lorenzen J.M. (2018). Noncoding RNAs in acute kidney injury. Kidney Int. 94, 870-881.

Deng L., Zhang W., Shi, Y. and Tang Y. (2019). Fusion of multiple heterogeneous networks for predicting circRNA-disease associations. Sci. Rep. 9, 9605.

Fan X., Weng X., Zhao Y., Chen W., Gan T. and Xu D. (2017). Circular RNAs in Cardiovascular Disease: An Overview. Biomed. Res. Int. 2017, 5135781.

Haque S. and Harries L.W. (2017). Circular RNAs (circRNAs) in health and disease. Genes (Basel) 8, 353.

Hu Y., Zhu H., Bu L. and He D. (2019). Expression profile of circular RNA s in TMJ osteoarthritis synovial tissues and potential functions of hsa_circ_0000448 with specific back-spliced junction. Am. J. Transl. Res. 11, 5357-5374.

Jackson R.J. and Standart N. (2007). How do microRNAs regulate gene expression?. Sci. STKE 2007, re1.

Kristensen L.S., Hansen T.B., Venø M.T. and Kjems J. (2018). Circular RNAs in cancer: opportunities and challenges in the field. Oncogene 37, 555-565.

Li B.F., Zhang Y., Xiao J., Wang F., Li M., Guo X.Z., Xie H.B. and Chen B. (2017a). Hsa_circ_0045714 regulates chondrocyte proliferation, apoptosis and extracellular matrix synthesis by promoting the expression of miR-193b target gene IGF1R. Hum. Cell 30, 311-318.

Li T.R., Jia Y.J., Wang Q., Shao X.Q. and Lv R.J. (2017b). Circular RNA: a new star in neurological diseases. Int. J. Neurosci. 127, 726-734.

Li Z., Ruan Y., Zhang H., Shen Y., Li T. and Xiao B. (2019). Tumor-suppressive circular RNAs: Mechanisms underlying their suppression of tumor occurrence and use as therapeutic targets. Cancer Sci. 110, 3630-3638.

Nelson A.E. (2018). Osteoarthritis year in review 2017: clinical. Osteoarthritis Cartilage 26, 319-325.

Ng W.L., Mohd Mohidin T.B. and Shukla K. (2018). Functional role of circular RNAs in cancer development and progression. RNA Biol. 15, 995-1005.

Park S.J., Cheon E.J., Lee M.H. and Kim H.A. (2013). MicroRNA-127-5p regulates matrix metalloproteinase 13 expression and interleukin-1β-induced catabolic effects in human chondrocytes. Arthritis Rheum. 65, 3141-3152.

Parra-Torres N.M., Cázares-Raga F.E. and Kouri J.B. (2014). Proteomic analysis of rat cartilage: the identification of differentially expressed proteins in the early stages of osteoarthritis. Proteome Sci. 12, 55.

Qu S., Yang X., Li X., Wang J., Gao Y., Shang R., Sun W., Dou K. and Li H. (2015). Circular RNA: A new star of noncoding RNAs. Cancer Lett. 365, 141-148.

Shu X., Cheng L., Dong Z. and Shu S. (2019). Identification of circular RNA-associated competing endogenous RNA network in the development of cleft palate. J. Cell Biochem. 120, 16062-16074.

Tang X., Wang S., Zhan S., Niu J., Tao K., Zhang Y. and Lin J. (2016). The prevalence of symptomatic knee osteoarthritis in china: Results from the china health and retirement longitudinal study. Arthritis Rheumatol. 68, 648-653.

Tu M., Li Y., Zeng C., Deng Z., Gao S., Xiao W., Luo W., Jiang W., Li L. and Lei G. (2016). MicroRNA-127-5p regulates osteopontin expression and osteopontin-mediated proliferation of human chondrocytes. Sci. Rep. 6, 25032.

Wang Y., Wu C., Zhang F., Zhang Y., Ren Z., Lammi M.J. and Guo X. (2019). Screening for differentially expressed circular RNAs in the cartilage of osteoarthritis patients for their diagnostic value. Genet. Test Mol. Biomarkers. 23, 706-716.

Wu Y., Zhang Y., Zhang Y. and Wang J.J. (2017). CircRNA hsa_circ_0005105 upregulates NAMPT expression and promotes chondrocyte extracellular matrix degradation by sponging miR-26a. Cell Biol. Int. 41, 1283-1289.

Xiao K., Xia Z., Feng B., Bian Y., Fan Y., Li Z., Wu Z., Qiu G. and Weng, X. (2019). Circular RNA expression profile of knee condyle in osteoarthritis by illumina HiSeq platform. J. Cell Biochem. 120, 17500-17511.

You Y., Wen R., Pathak R., Li A., Li W., St Clair D., Hauer-Jensen M. Zhou D. and Liang Y. (2014). Latexin sensitizes leukemogenic cells to gamma-irradiation-induced cell-cycle arrest and cell death through Rps3 pathway. Cell Death Dis. 5, e1493.

Yu F., Xie C., Sun J., Feng H. and Huang X. (2018). Circular RNA expression profiles in synovial fluid: a promising new class of diagnostic biomarkers for osteoarthritis. Int. J. Clin. Exp. Pathol. 11, 1338-1346.

Zhao S.Y., Wang J., Ouyang S.B., Huang Z.K. and Liao L. (2018). Salivary circular RNAs Hsa_Circ_0001874 and Hsa_Circ_0001971 as novel biomarkers for the diagnosis of oral squamous cell carcinoma. Cell Physiol. Biochem. 47, 2511-2521.

Zhou Z.B., Huang G.X., Fu Q., Han B., Lu J.J., Chen A.M. and Zhu L. (2019). circRNA.33186 contributes to the pathogenesis of osteoarthritis by sponging miR-127-5p. Mol. Ther. 27, 531-541.

Accepted March 5, 2021